POLITECNICO DI TORINO
Repository ISTITUZIONALE

Multi-Objective Hybrid Electric Vehicle Control for Maximizing Fuel Economy and Battery Lifetime

Original
Multi-Objective Hybrid Electric Vehicle Control for Maximizing Fuel Economy and Battery Lifetime / Anselma, P.G., Kollmeyer, P., Belingardi, G., Emadi, A.. - (2020), pp. 525-530. (2020 IEEE Transportation Electrification Conference & Expo (ITEC) 23-26 June 2020) [10.1109/ITEC48692.2020.9161518].

Availability:
This version is available at: 11583/2843466 since: 2020-09-02T14:04:49Z

Publisher:
IEEE

Published
DOI:10.1109/ITEC48692.2020.9161518

Terms of use:

This article is made available under terms and conditions as specified in the corresponding bibliographic description in the repository

Publisher copyright
IEEE postprint/Author's Accepted Manuscript

©2020 IEEE. Personal use of this material is permitted. Permission from IEEE must be obtained for all other uses, in any current or future media, including reprinting/republishing this material for advertising or promotional purposes, creating new collecting works, for resale or lists, or reuse of any copyrighted component of this work in other works.

(Article begins on next page)

16 September 2026

Multi-Objective Hybrid Electric Vehicle Control for Maximizing Fuel Economy and Battery Lifetime

Pier Giuseppe Anselma[1,2,3], Phillip Kollmeyer[3], Giovanni Belingardi[1,2], Ali Emadi[3]
[1]Department of Mechanical and Aerospace Engineering (DIMEAS), Politecnico di Torino, Torino, Italy
[2]Center for Automotive Research and Sustainable Mobility (CARS), Politecnico di Torino, Torino, Italy
[3]McMaster Automotive Resource Center (MARC), McMaster University, Hamilton, ON, Canada

E-mail: pier.anselma@polito.it

***Abstract*- High voltage batteries are a fundamental component of hybrid electric vehicles (HEVs). Energy management strategies (EMSs) for HEVs generally aim at maximizing fuel economy solely, yet the method of hybrid powertrain control has a strong impact on the battery lifetime. This paper proposes a multi-objective formulation of dynamic programming, a popular off-line optimization tool, which is capable of maximizing both fuel economy and battery lifetime. Obtained numerical results allow correlation of predicted fuel economy with the corresponding predicted battery lifetime. The developed tool can thus help engineers account for battery lifetime during both the HEV powertrain architecture design and the EMS calibration processes.**

I. INTRODUCTION

Hybrid electric vehicles (HEVs) are a promising technology within the field of transportation electrification and their adoption in the global vehicle market is forecasted to intensify over the next few years [1]. Development processes of HEVs include the implementation of dedicated energy management strategies (EMSs), also known as hybrid supervisory controllers. These controllers perform vehicle-level management tasks involving the repartition of requested power from the driver among components of the hybrid electric powertrain. Moreover, they aim to effectively supervise some fundamental vehicle states such as the battery state-of-charge (SOC), the overall fuel consumption and the emission of pollutants. In general, two opposite categories of EMSs for HEVs can be identified, namely off-line strategies and on-line strategies. Off-line EMSs exploit the knowledge of the entire vehicle speed profile for examined driving missions to control the operation of the HEV powertrain according to specific optimization criteria [2]. They can be used for a wide range of purposes that involve assessing ideal fuel economy capabilities when designing and sizing HEV powertrains, supporting the optimal calibration of on-line EMSs and providing an optimal benchmark for on-line EMSs as well. On the other hand, on-line EMSs do not need the knowledge of the entire driving mission in advance, therefore they can find straightforward implementation in the on-board electronic control unit of HEVs.

Both the off-line and on-line EMSs presented above are usually designed to maximize a performance single-objective, the vehicle's fuel economy which is proportionally linked to tailpipe emissions. In this framework, the HEV battery working conditions are controlled with the simple target of performing charge-sustaining (CS) operation over a drive cycle or mission. The impact of EMS operation on other HEV battery conditions, such as its expected lifetime, is therefore usually neglected. Nevertheless, battery lifetime has a crucial impact on several aspects of HEVs including total cost of ownership and maintenance [3]. This suggests that research activities should aim not only at the experimental verification [4] and on-board estimation of battery ageing effects [5], but also at including battery lifetime considerations in both off-line and on-line EMSs at early development stages of HEVs.

Several HEV EMS control strategies which consider battery ageing have been proposed in the literature. For real-time EMSs, the current most popular battery state-of-health (SOH) sensitive HEV powertrain control approach utilizes the equivalent consumption minimization strategy (ECMS) [6]. An ECMS which considers battery SOH must have two equivalent fuel consumption terms, i.e. (1) an equivalent fuel term representing the usage of battery energy, as implemented in the standard formulation of the ECMS, and (2) an equivalent fuel term representing the battery lifetime consumption. Such multi-objective adaptations of the ECMS have been developed for parallel HEVs with automatic manual transmissions [7][8] and continuously variable transmissions [9]. Convex optimization is another example of real-time EMS approach for HEVs, and its effectiveness has been suggested when considering battery SOH as additional control target for a plug-in hybrid electric city bus as well [10].

Little work has been done regarding battery lifetime oriented off-line EMSs for HEVs though. In 2013, a stochastic dynamic programming (DP) formulation was implemented for a power-split HEV considering anode side resistive film formation and amp-hours processed as the battery SOH metrics [11]. In 2016, a two-point optimization problem was solved using DP for a plug-in HEV while retaining an application-specific target battery life as objective of the HEV EMS [12]. In the authors' opinion, the limited amount of research on off-line battery SOH-aware EMSs for HEVs motivates further contribution to cover the topic more extensively. This paper therefore aims at introducing a multi-objective formulation for DP, the most popular off-line EMS for HEVs, which considers both fuel economy and battery lifetime. The rest of the paper is organized as follows: the macro-scale battery ageing model

retained from literature is firstly presented. Then, the HEV powertrain model under consideration is illustrated. The operating principle of DP is recalled and its multi-objective formulation is detailed. Finally, results and conclusions are given.

II. Macroscale Battery Ageing Model

In this paper, a throughput-based macroscale battery capacity fade model from [7] is employed. This numerical model supposes that a specific amount of charge throughput, which is a function of the current magnitude and temperature of the charge / discharge cycles, can be provided by the battery under steady operating conditions before reaching its end-of-life. Compared to more complex battery ageing models (e.g. electrochemical models and event-based models), throughput-based ageing models exhibit significantly improved computational efficiency [13]. For this reason, they seem to be the most suitable battery ageing models to be implemented in optimization based off-line HEV EMSs as these usually are computationally demanding [14].

The SOH of the high-voltage battery at the generic time instant t_i can be defined according to (1):

$$SOH(t_i) = SOH_0 - \frac{1}{\int_0^{t_i} \frac{N(c,T)}{c} dt} \quad (1)$$

where SOH_0 denotes the initial SOH (equal to 1). c represents the instantaneous battery C-rate, which is defined as the ratio between the current in amps and the battery capacity in amp-hours. N is the number of roundtrip cycles before the battery reaches its end-of-life and it is not a constant value, rather it depends on the battery operating conditions (i.e. C-rate, temperature T). In general, the battery reaches its end-of-life as SOH approaches zero and the battery has no remaining capacity. In order to determine N, the percentage of battery capacity loss $\Delta Ah_{batt\%}$ needs to be characterized by following the approach proposed by Bloom et al. in 2001 [15]. This takes inspiration from the Arrhenius equation describing the behavior of ideal gases. However, the general equation has been modified as follows in order to apply it to battery ageing:

$$\Delta Ah_{batt\%} = B(c) \cdot e^{-\frac{A_f(c)}{T}} \cdot {Ah_{tp}}^z \quad (2)$$

Following (2), $\Delta Ah_{batt\%}$ depends on an empirical pre-exponential factor B, the ageing factor A_f, the lumped cell temperature T, a power-law factor z and the total throughput Ah_{tp} in ampere-hour. Here, both B and A_f are a function of the instantaneous battery c-rate c. The numerical values for parameters of an A123 26650 cell are obtained from [7], where the authors declared that the numerical model was in turn tuned according to data published in [16]. Table I reports the parameter values utilized here, including the pre-exponential factor B tabulated with respect to c. The lumped cell temperature is assumed to be a constant value of 25°C (i.e. the battery conditioning system maintains this temperature). Battery SOC dependent parameters can be directly derived from the constant power discharge characteristics in the cell manufacturer catalogue [17].

TABLE I
Battery Ageing Parameters for a A123 ANR26650 cell

Parameter	Value	Units of measure
Ageing factor, A_f	3,814.7 – 44.6·c	K
Power law factor, z	0.55	-
Temperature, T	298	K
Empirical pre-exponential factor $B(c)$	[28,314 ; 21,681 ; 12,934 ; 15,512]	-
Current C-rate, c	[1; 2; 6; 10]	-

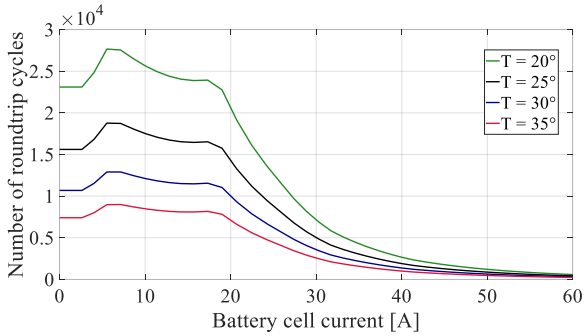

Fig. 1 Number of allowed roundtrip cycles as a function of the battery cell current and the temperature according to the considered ageing model.

For the modeling it is assumed that the end of the HEV battery lifetime corresponds to a loss of 20% of its initial capacity, so a value of 20% is used for $\Delta Ah_{batt\%}$. By using this information and solving (2) for $Ah_{tp}(c)$, it becomes possible to calculate the total number of roundtrip cycles N allowed for the battery lifetime as function of the c-rate in (3). N can in turn be considered in (1) to evaluate the rate of battery SOH.

$$N(c,T) = \frac{Ah_{tp}(c,T)}{2 \cdot Ah_{batt}} \quad (3)$$

Ah_{batt} is the battery energy capacity in ampere-hours. The factor of two in the denominator allows the model to account for both charging and discharging phases in the battery roundtrip cycles. The number of allowed roundtrip cycles as predicted by the described ageing model is illustrated in Fig. 1 as a function of the battery cell current and its temperature. Predicting the residual battery lifetime becomes thus possible using the described model. Here, it is assumed that all the cells of the battery pack are identical and they exhibit the same state conditions such as SOC and SOH as example, i.e. the battery management system operates a uniform load distribution among cells at each time instant. As an additional hypothesis, the battery ageing model is assumed here to be independent from the battery SOC value. This is likely the case for this application because the HEV powertrain is controlled to operate in CS mode, where the battery SOC undertakes a narrow span of values.

III. HEV powertrain model

The HEV powertrain architecture used for this study is the same as the third generation Toyota Prius® hybrid. This power-split HEV powertrain, as shown in Fig. 2 through

TABLE II
MODELED HEV PARAMETERS

Component	Parameter	Value
Vehicle	Mass	1531 kg
ICE	Capacity	1.8 L
	Power max	72 kW @ 5,000 rpm
	Torque max	142 Nm @ 4,000 rpm
MG1	Power max	42 kW
MG2	Power max	65 kW
Transmission ratios	i_{PG1} ($Ring_1$ / Sun_1)	2.6
	i_{PG2} ($Ring_2$ / Sun_2)	0.26
	i_{FD}	3.27
Auxiliaries	Electrical subsystem power	500 W
Battery	Pack capacity	1.52 kWh
	Pack configuration	100S – 2P
	Cell type & capacity	A123 26650, 2.2Ah

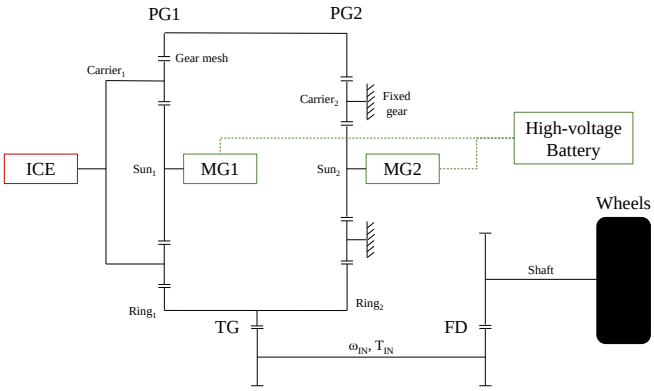

Fig. 2 Toyota Prius hybrid electric powertrain scheme.

mechanical symbols, is a well-known layout and open source data regarding it are available [18]. An HEV model is developed and the parameters used for it, as defined in in Table II, are similar to the Prius. The main difference is that a 1.52 kWh battery pack consisting of 100 series and 2 parallel connected A123 26650 cells, the cells for which the ageing model in section II is developed, is utilized. Two planetary gear (PG) sets are embedded in the power-split HEV that regulate the kinematic relationships between different power components, namely an internal combustion engine (ICE) and two electric motor/generators (MGs). This powertrain layout features two operating modes, hybrid or pure electric, depending on whether the ICE is activated or not. Pure electric mode only utilizes MG2 and can be employed during braking events for example to recover electrical energy and store it in the battery.

The HEV powertrain is modeled using a backward quasi-static approach for deriving the requested power values and speed of components directly from the driving mission requirements [14]. The value of required torque at the input shaft of the final drive T_{IN} is determined at each time instant of the driving mission as

$$T_{IN} = \frac{(F_{roll}+F_{misc}+F_{aero}+m_{veh}\cdot\ddot{x})\cdot r_{dyn}}{i_{FD}} \quad (4)$$

where m_{veh}, $\ddot{x}$, r_{dyn} and i_{FD} respectively represent the vehicle mass, the vehicle acceleration, the wheel rolling radius and the final drive ratio. F_{roll}, F_{misc} and F_{aero} are resistive load terms provided by the rolling resistance, some miscellaneous terms (e.g. transmission losses, side forces, road slope) and aerodynamic drag, respectively.

As it can be observed from Fig. 2, the MG2 angular speed ω_{MG2} is proportionally constrained to the angular speed of the final drive input shaft ω_{in}, while the MG1 angular speed ω_{MG1} depends on the ICE speed ω_{ICE} as well. Assuming a 1:1 transmission ratio for the transfer gearset (TG) in Fig. 2, the resulting kinematic constraints for the hybrid electric drivetrain can then be outlined as:

$$\begin{bmatrix}\omega_{MG1}\\ \omega_{MG2}\end{bmatrix} = \begin{bmatrix}-i_{PG_1} & i_{PG_1}+1\\ i_{PG_2}+1 & 0\end{bmatrix}\begin{bmatrix}\omega_{IN}\\ \omega_{ICE}\end{bmatrix} \quad (5)$$

where i_{PG1} and i_{PG2} represent the ratio between number of teeth for the ring gear and the number of teeth for the sun gear for PG1 and PG2, respectively. Based on the torque ratios for standard epicyclic gearing, and assuming unitary efficiency for the transmission system, torque values for both MG1 (T_{MG1}) and MG2 (T_{MG2}) can be derived according to the torque request coming from road and driver (T_{IN}) and the torque of the ICE (T_{ICE}), which is used as the control variable in (6).

$$\begin{bmatrix}T_{MG1}\\ T_{MG2}\end{bmatrix} = \begin{bmatrix}0 & -\frac{1}{i_{PG1}+1}\\ \frac{i_{PG2}+1}{i_{PG2}} & -\left(\frac{i_{PG1}}{i_{PG1}+1}\right)\cdot\left(\frac{i_{PG_2}+1}{i_{PG_2}}\right)\end{bmatrix}\begin{bmatrix}T_{IN}\\ T_{ICE}\end{bmatrix} \quad (6)$$

As concerns the electrical energy path, the amount of power that the battery is requested to either deliver or absorb (P_{batt}) is calculated as:

$$P_{batt} = \left(\sum_{i=1}^{2}\frac{P_{MGi}}{[\eta_{MGi}(\omega_{MGi},T_{MGi})]^{sign(P_{MGi})}}\right) + P_{aux} \quad (7)$$

where P_{MG} and η_{MG} respectively represent the mechanical power and the overall efficiency of an MG, which is evaluated by means of empirical lookup tables with speed and torque as independent variables. Utilizing the sign of P_{MG} as exponent in the denominator allows capturing both depleting and charging battery conditions within this formula. Finally, P_{aux} is the power requested by the accessories (e.g. lubrication, air conditioning) and is assumed having a constant value here. The change in battery SOC for a timestep is then be evaluated by considering an equivalent open circuit model as in (8):

$$\dot{SOC} = \frac{V_{OC}(SOC)-\sqrt{[V_{OC}(SOC)]^2-4\cdot R_{IN}(SOC)\cdot P_{batt}}}{2\cdot R_{IN}(SOC)}\cdot\frac{n_P}{Ah_{batt}\cdot 3600} \quad (8)$$

where R_{IN} is the internal resistance of the battery pack, as obtained by interpolating in 1D lookup tables with SOC ad independent variable. n_P stands for the number of cells in parallel as given by the battery pack configuration.

Concerning the ICE, the instantaneous rate of fuel consumption can be finally evaluated using an empirical steady-state lookup table with torque and speed as independent variables.

IV. MULTI-OBJECTIVE HEV CONTROL

This section details the multi-objective formulation of DP which is implemented to find an optimal solution for the HEV off-line control problem.

A. Multi-objective off-line HEV control problem

The mathematical expression of the HEV off-line control problem formulated here is reported in (9):

$$\min\left\{J=\int_{t_0}^{t_{end}}\mathrm{L}(t)dt\right\}$$

subject to:

$$\begin{gathered}SOC(t_0)=SOC(t_{end})\\ \omega_{ICE\,min}\le\omega_{ICE}\le\omega_{ICE\,MAX}\\ \omega_{MG1\,min}\le\omega_{MG1}\le\omega_{MG1\,MAX}\\ \omega_{MG2\,min}\le\omega_{MG2}\le\omega_{MG2\,MAX}\\ T_{ICE\,min}\le T_{ICE}\le T_{ICE\,MAX}\\ T_{MG1\,min}\le T_{MG1}\le T_{MG1\,MAX}\\ T_{MG2\,min}\le T_{MG2}\le T_{MG2\,MAX}\\ SOC_{min}\le SOC\le SOC_{MAX}\\ SOH_0=1\end{gathered}\tag{9}$$

where $L(t)$ is the instantaneous cost function is minimized throughout the driving mission. The battery SOC is set to be the same at the beginning and end of the considered driving missions, ensuring that charge is sustained. Finally, both battery SOC, speeds (ω) and torques (T) are restricted within the corresponding allowed operating regions. The initial battery SOH is set to 1 in order to consider non-aged battery conditions. The explicit formulation of L is as follows:

$$\begin{aligned}L(t)=\left[\dot{m}_{fuel}+m_{fuel-crank}\cdot(start_{ICE}>0)\right]\\ \cdot\,\$_{fuel}+\alpha_{batt}\cdot\$_{batt}\cdot\dot{SOH}\end{aligned}\tag{10}$$

where $\dot{m}_{fuel}$ and $m_{fuel-crank}$ represent the fuel mass rate at each time instant in which the ICE operates and the amount of fuel mass needed to crank the ICE throughout starting events, respectively. The parameter $start_{ICE}$ defines a binary variable detecting ICE start occurrence. The variables $\$_{fuel}$ and $\$_{batt}$ represent cost values for fuel and for the battery, respectively. $\$_{fuel}$ is based on the November 2019 averaged US gasoline price of 2.62 $/gallon [19], while a value of $3,000 is used for $\$_{batt}$ from [20]. $\dot{SOH}$ is the instantaneous rate of battery SOH, while α_{batt} denotes a scaling coefficient for the illustrated battery ageing model which is used to tune the value of fuel versus the battery. The higher the α_{batt} value, the more battery ageing is minimized at the expense of fuel economy.

The set of control variables U contain speed and torque values for the ICE as formulated in (11).

$$U=\begin{Bmatrix}\omega_{ICE}\\ T_{ICE}\end{Bmatrix}\tag{11}$$

As illustrated in the previous section, the reported set of control variables is sufficient for determining the operating conditions of all the remaining power components of the electrified powertrain.

B. Dynamic Programming formulation

In general, DP is an optimization approach that solves the control problem for dynamic systems by exhaustively exploring all the possible control actions backwardly at each time step. DP is popular for solving HEV off-line control problems because it effectively returns a global optimal solution. The minimum overall value of the predefined cost function, corresponding to the global optimal solution, is determined by sweeping discretized values for control and state variables of the analyzed control problem at each time step [21]. While control variables for the multi-objective control problem have been outlined in the previous paragraph, related state variables still need definition. The DP states are, by definition, the parameters which are a function of the preceding time steps, and consist of X for this system:

$$X=\begin{Bmatrix}SOC\\ ICE_{on/off}\end{Bmatrix}\tag{12}$$

where battery SOC is a state because it is the integral of the battery current , the ICE state (i.e. on/off) is included because cranking events are only allowed at a certain frequency so the comfort of the ride is reasonable. A third state variable term could theoretically be considered here for the battery SOH, but since this value changes very slowly and DP solution time increases exponentially with additional state variable terms it was decided to be unnecessary.

V. RESULTS

The simulation results obtained by implementing the described EMS algorithm are presented in this section. Six driving missions were used including both standard drive cycles (UDDS, HWFET, WLTP, US06) and real-world driving missions recorded by the authors including the extra-urban uphill (RWC uphill) and extra-urban downhill (RWC downhill) driving conditions respectively [22]. All the listed driving missions have been simulated for the considered power-split hybrid electric powertrain while being controlled off-line by the multi-objective DP approach. Thirty elements are used for the DP grid for each control variable. Approximately 40 minutes is required for the DP algorithm to run on a desktop computer with Intel Core i7-8700 (3.2 GHz) and 32 GB of RAM.

Several simulations are performed for each driving mission, with α_{batt} ranging from zero (optimization goal OG: fuel economy only) to a value large enough to achieve a battery lifetime of around 350,000 km. The battery lifetime is determined by assuming the corresponding driving mission is steadily repeated until battery capacity has decreased by 20%. Fig. 3 illustrates the optimal operating power of the components of the HEV powertrain in a selected portion of WLTP as predicted by DP considering fuel economy as OG. On the other hand, optimal time series of battery power and battery SOC are compared in Fig. 4 considering fuel economy, 150k km battery lifetime and 300k km battery lifetime as OGs in US06, respectively. The battery lifetime and normalized fuel economy for each modeled value of α_{batt} is finally plotted in

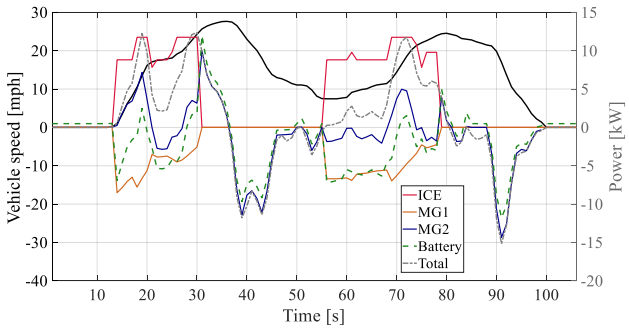

Fig. 3 HEV operation predicted by DP for selected portion of WLTP.

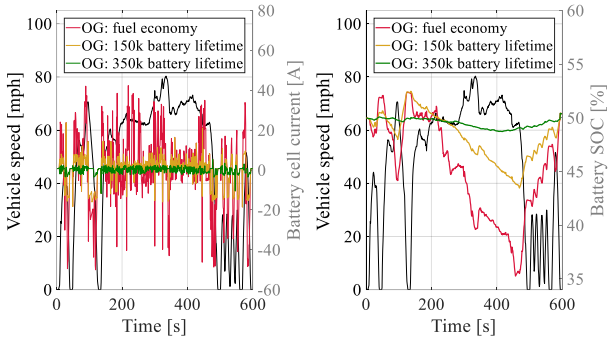

Fig. 4 Battery power and SOC as predicted by the multi-objective DP in US06 for different optimization goals.

Fig. 5, showing that when optimizing for greater fuel economy the battery lifetime can be reduced substantially. For example for the WLTP profile, an increase in fuel economy of around 7% reduces the battery lifetime to just 80,000 km. Table III reports numerical values for some key points of Pareto frontiers for each modeled driving mission. Finally, HEV operational statistics such as the root mean square (RMS) of battery cell current, friction brake energy, fuel economy, ICE deactivation time and average efficiency are compared between key points of the Pareto frontiers for all the driving missions in Fig. 6.

Looking at results obtaind for the power-split HEV in Fig. 5 and Table III, the predicted battery lifetime in correspondence with $\alpha_{batt} = 0$, where the optimization only targets fuel economy, is below 100,000 km for all the considered driving missions. Battery lifetime can be increased to 300,000 km or more, a suitable design lifetime, by progressively increasing α_{batt} to place more value on battery lifetime. The steeper the Pareto frontier is for a driving mission in Fig. 5, the more beneficial the adopted optimization approach is in extending the predicted battery lifetime while limiting the increase in fuel consumption. As an example, for the WLTP and HWFET cycles the control algorithm can achieve around a four fold increase in battery lifetime with a corresponding fuel consumption increase of 5.5 % and 1.9 %, respectively.

The increase in fuel consumption when progressively extending battery lifetime can be traced back to three main factors as illustrated in Fig. 6, including (1) the increase in the usage of friction brakes to decelerate the HEV to reduce high values of battery current which result in more ageing, (2) the increase in the overall on time of the ICE due to the need to balance the power flow in the system with less battery usage and hence reduced battery ageing, and (3) the reduction of ICE overall efficiency when changing its operational conditions in order to preserve battery lifetime. Finally, the results illustrated in Fig. 6 show that battery cell RMS current decreases substantially as battery lifetime is increased, which correlates with the battery ageing plot in Fig. 1.

VI. CONCLUSIONS

Battery lifetime is an important aspect to be considered when designing EMSs for HEVs. A multi-objective off-line EMS for HEVs was developed, which utilizes dynamic programming and accounts for both fuel economy and battery lifetime. The developed method was applied to a power-split electrified powertrain and allows prediction of the battery lifetime for different predefined driving missions. Consideration of battery ageing in the control method is shown to greatly increase battery lifetime while having a minor effect

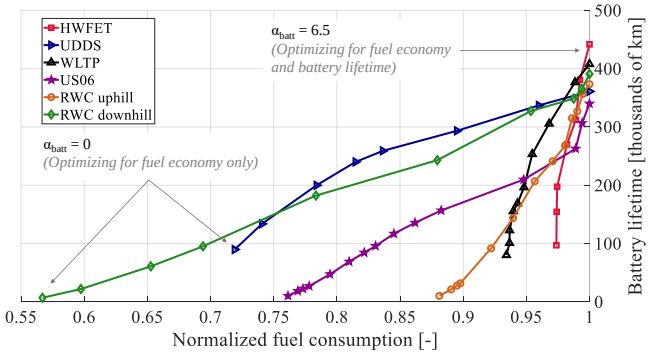

Fig. 5 Pareto frontiers for the multi-objective DP over different driving missions.

TABLE III
DP RESULTS FOR FUEL ECONOMY AND BATTERY LIFETIME

Driving mission	**Point #1** ($\alpha_{battery}$ = 0) *Tuned for fuel economy only*		**Point #2** ($\alpha_{battery}$ = 0.01 to 0.5) *Tuned for ≈150k km lifetime*		**Point #3** ($\alpha_{battery}$ = 0.5 to 6.5) *Tuned for ≈350k km lifetime*	
	Fuel economy (mpg)	Battery lifetime (thousands of km)	Fuel economy (mpg)	Battery lifetime (thousands of km)	Fuel economy (mpg)	Battery lifetime (thousands of km)
HWFET	74.8	97	74.8 *(-0.0 %)*	154 *(x 1.6)*	73.4 *(-1.9 %)*	381 *(x 3.9)*
UDDS	90.0	90	86.2 *(-4.2 %)*	149 *(x 1.7)*	64.7 *(- 28.1%)*	361 *(x 4.0)*
WLTP	66.7	80	66.3 *(-0.6 %)*	155 *(x 1.9)*	63.0 *(-5.5 %)*	376 *(x 4.7)*
US06	56.6	10	48.8 *(-13.7 %)*	157 *(x 15.3)*	43.1 *(-23.9 %)*	340 *(x 33.1)*
RWC_uphill	45.8	10	43.0 *(-6.2 %)*	144 *(x 14.1)*	40.4 *(-11.9 %)*	373 *(x 36.7)*
RWC_downhill	102.2	7	73.9 *(-27.6 %)*	182 *(x 26.2)*	57.9 *(-43.3 %)*	391 *(x 56.1)*

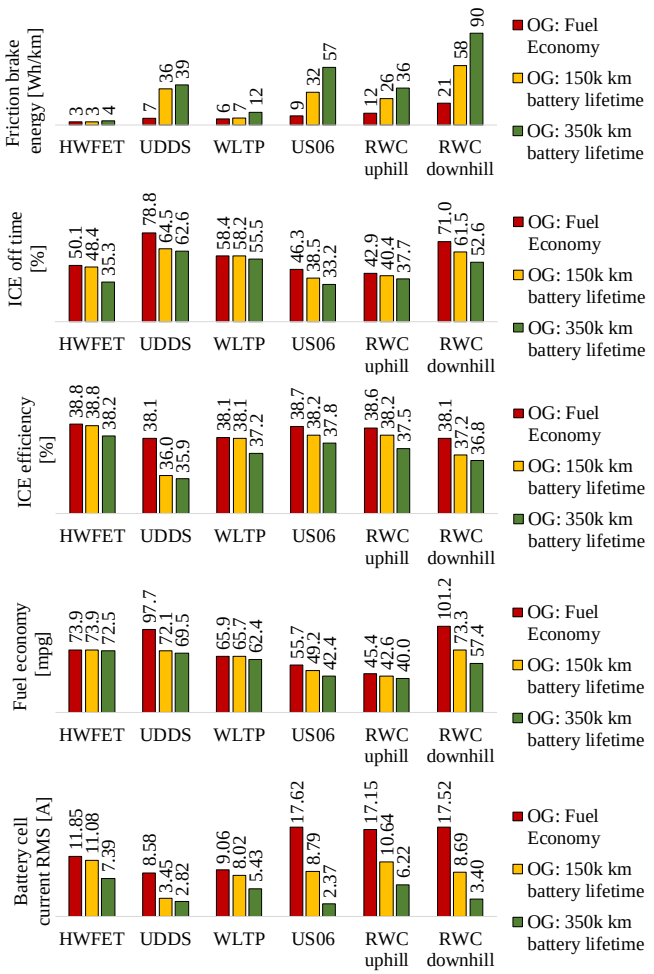

Fig. 6 HEV operational statistics for the multi-objective DP.

on fuel economy in many cases. For example a 1.9 times increase in battery lifetime and only a 0.6% reduction in fuel economy was achieved for the WLTP cycle for one optimization tuning case. A range of results are observed when tuning the optimization goals to achieve 350k km battery lifetime, with a reduction in fuel economy compared to the fuel economy only optimization case of between 1.9 and 43.4% for the six drive cycles investigated. This numerical approach could be implemented in HEV design methodologies, allowing designers to develop control algorithms with a suitable trade-off between fuel economy and battery lifetime.

REFERENCES

[1] B. Bilgin et al., "Making the Case for Electrified Transportation," in *IEEE Transactions on Transportation Electrification*, vol. 1, no. 1, pp. 4-17, 2015.

[2] A. Biswas and A. Emadi, "Energy Management Systems for Electrified Powertrains: State-of-the-Art Review and Future Trends," in *IEEE Transactions on Vehicular Technology*, vol. 68, no. 7, pp. 6453-6467, July 2019.

[3] R. Ahmed, M. E. Sayed, I. Arasaratnam, J. Tjong and S. Habibi, "Reduced-Order Electrochemical Model Parameters Identification and SOC Estimation for Healthy and Aged Li-Ion Batteries Part I: Parameterization Model Development for Healthy Batteries," in *IEEE Journal of Emerging and Selected Topics in Power Electronics*, vol. 2, no. 3, pp. 659-677, Sept. 2014.

[4] P. J. Kollmeyer, T. M. Jahns, "Ageing and performance comparison of absorbed glass matte, enhanced flooded, PbC, NiZn, and LiFePO4 12V start stop vehicle batteries", *J. Power Sources*, vol. 441, 2019.

[5] A. Bonfitto, E. Ezemobi, N. Amati, S. Feraco, A. Tonoli and S. Hegde, "State of Health Estimation of Lithium Batteries for Automotive Applications with Artificial Neural Networks," *2019 AEIT International Conference of Electrical and Electronic Technologies for Automotive (AEIT AUTOMOTIVE)*, Torino, Italy, 2019, pp. 1-5.

[6] P. Pisu and G. Rizzoni, "A Comparative Study Of Supervisory Control Strategies for Hybrid Electric Vehicles," in *IEEE Transactions on Control Systems Technology*, vol. 15, no. 3, pp. 506-518, May 2007.

[7] S. Ebbesen, P. Elbert and L. Guzzella, "Battery State-of-Health Perceptive Energy Management for Hybrid Electric Vehicles," in *IEEE Transactions on Vehicular Technology*, vol. 61, no. 7, pp. 2893-2900, Sept. 2012.

[8] Li, J., Huber, T., and Beidl, C., "Predictive Multi-Objective Operation Strategy Considering Battery Cycle Ageing for Hybrid Electric Vehicles," *SAE Int. J. Alt. Power.* 7(3):217-232, 2018.

[9] L. Tang, G. Rizzoni and S. Onori, "Energy Management Strategy for HEVs Including Battery Life Optimization," in *IEEE Transactions on Transportation Electrification*, vol. 1, no. 3, pp. 211-222, Oct. 2015.

[10] S. Xie, X. Hu, Q. Zhang, X. Lin, B. Mu, H. Ji, "Aging-aware co-optimization of battery size, depth of discharge, and energy management for plug-in hybrid electric vehicles", *Journal of Power Sources*, Vol. 450, 2020.

[11] S. J. Moura, J. L. Stein and H. K. Fathy, "Battery-Health Conscious Power Management in Plug-In Hybrid Electric Vehicles via Electrochemical Modeling and Stochastic Control," in *IEEE Transactions on Control Systems Technology*, vol. 21, no. 3, pp. 679-694, 2013.

[12] C. Patil, P. Naghshtabrizi, R. Verma, Zhijun Tang, K. Smith and Ying Shi, "Optimal battery utilization over lifetime for parallel hybrid electric vehicle to maximize fuel economy," *2016 American Control Conference (ACC)*, Boston, MA, 2016, pp. 1524-1529.

[13] Vora, A. P., Jin, X., Hoshing, V., Shaver, G., Varigonda, S., & Tyner, W. E., "Integrating battery degradation in a cost of ownership framework for hybrid electric vehicle design optimization", *Proc IMeche, Part D: J Automobile Engineering*, online 21 Oct. 2018.

[14] P. G. Anselma, Y. Huo, J. Roeleveld, G. Belingardi and A. Emadi, "Slope-Weighted Energy-Based Rapid Control Analysis for Hybrid Electric Vehicles," in *IEEE Transactions on Vehicular Technology*, vol. 68, no. 5, pp. 4458-4466, May 2019.

[15] I. Bloom, B. W. Cole, J. J. Sohn, S. A. Jones, E. G. Polzin, V. S. Battaglia, G. L. Henriksen, C. Motloch, R. Richardson, T. Unkelhaeuser, D. Ingersoll, and H. L. Case, "An accelerated calendar and cycle life study of Li-ion cells," *J. Power Sources*, vol. 101, no. 2, pp. 238–247, Oct. 2001.

[16] J. Wang, P. Liu, J. Hicks-Garner, E. Sherman, S. Soukiazian, M. Verbrugge, H. Tataria, J. Musser, and P. Finamore, "Cycle-life model for graphite- LiFePO4 cells," *J. Power Sources*, vol. 196, no. 8, pp. 3942– 3948, Apr. 2011.

[17] A123 systems, "Nanophosphate® High Power LithiumIon Cell ANR26650M1-B", [online] https://www.batteryspace.com/prod-specs/6610.pdf (accessed 19 November 2019).

[18] Kim, N., Rousseau, A., and Rask, E., "Autonomie Model Validation with Test Data for 2010 Toyota Prius," *SAE Technical Paper* 2012-01-1040, 2012.

[19] US Department of Energy, "eGallon: Compare the costs of driving with electricity", [online] https://www.energy.gov/maps/egallon (accessed 19 November 2019).

[20] L. Serrao, S. Onori, A. Sciarretta, Y. Guezennec and G. Rizzoni, "Optimal energy management of hybrid electric vehicles including battery ageing," *Proceedings of the 2011 American Control Conference*, San Francisco, CA, 2011, pp. 2125-2130.

[21] J. Lempert, B. Vadala, K. Arshad-Aliy, J. Roeleveld and A. Emadi, "Practical Considerations for the Implementation of Dynamic Programming for HEV Powertrains," *2018 IEEE Transportation Electrification Conference and Expo (ITEC)*, Long Beach, CA, 2018, pp. 755-760.

[22] P.G. Anselma, A. Biswas, L. Bruck et al., "Accelerated Sizing of a Power Split Electrified Powertrain", *SAE Technical Paper* 2020-01-0843, 2020.